# Two-Step Enhanced Deep Learning Approach for Electromagnetic Inverse Scattering Problems

He Ming Yao, *Student Member, IEEE*, Wei E. I. Sha, *Senior Member, IEEE*, and Lijun Jiang, *Fellow, IEEE*

***Abstract*—In this letter, a new deep learning (DL) approach is proposed to solve the electromagnetic inverse scattering (EMIS) problems. The conventional methods for solving inverse problems face various challenges including strong ill-conditions, high contrast, expensive computation cost, and unavoidable intrinsic nonlinearity. To overcome these issues, we propose a new two-step machine learning based approach. In the first step, a complex-valued deep convolutional neural network is employed to retrieve initial contrasts (permittivities) of dielectric scatterers from measured scattering data. In the second step, the previously obtained contrasts are input into a complex-valued deep residual convolutional neural network to refine the reconstruction of images. Consequently, the EMIS problem can be solved with much higher accuracy even for high-contrast objects. Numerical examples have demonstrated the capability of the newly proposed method with the improved accuracy. The proposed DL approach for EMIS problem serves a new path for realizing real-time quantitative microwave imaging for high-contrast objects.**

***Index Terms*—Convolutional neural network, electromagnetic inverse scattering (EMIS), high-contrast object, residual learning, two-step process.**

## I. Introduction

THE electromagnetic inverse scattering (EMIS) problem aims to obtain the imaging of scatterers from the knowledge of measured scattered fields information [1]–[3]. As a nondestructive detecting method, the EMIS only needs the scattered field information outside the object medium. In the past few decades, the EMIS has been widely applied in civil measurement and medical testing [4], [5]. For an EMIS problem, reconstruction algorithms like stochastic optimization methods [6]–[8] have been proposed. Meanwhile, a large number of new modeling methods, including Born iterative method [9], contrast source inversion [10], contrast-source extend Born [11], [12], and subspace optimization method [13] are also raised. However, all these conventional methods for an EMIS problem have to encounter ill-posedness [2], [3]. Besides, the dependence on the Green's function to construct electromagnetic (EM) coupled equations in conventional methods greatly limits their application in practical complex scenarios, where the Green's function has to be constructed case-by-case. The objects made of high contrast material also pose a challenge to conventional methods in terms of the accuracy. Plus, the high complexity and long computing time keep making inverse scattering problems a challenge in the real applications, especially for high contrast and large objects [2], [14].

The rapid development of deep learning (DL) approaches [15] has been pushing its application to computational electromagnetic (CEM). There have been numerous successful applications, including electromagnetic computation [16]–[18], remote sensing [19], [20], and field-circuit cosimulations [21], [22]. The artificial neural network has been proposed to solve the EMIS problem [23], [24], where a set of parameters like geometric properties are extracted. However, these methods become limited for arbitrary and inhomogeneous scatterers. Recently, other works related to deep neural network (DNN) have been proposed for solving EMIS problem [28]–[30]. Moreover, the learning-by-examples paradigm is also proposed to formulate various machine learning (ML) approaches to solve the EMIS problem [31]. In [25]–[27], the DL approaches are employed to improve the solving methods and obtain a better performance. However, these machine-learning based methods only use a one-step DL model that is based on the initial inputs only provided by the conventional methods, such as the backpropagation method [32].

In this letter, we propose a new two-step DL approach to solve the EMIS problems. The first step is based on the complex-valued deep convolutional neural network (DConvNet). It retrieves the initial permittivity images of dielectric scatterers from measured scattering data. In the second step, the complex-valued deep residual convolutional neural network (DRCNN) is employed to further extract features from the previously obtained permittivity image to improve the reconstruction. The advantages and innovative contribution of the proposed method are: 1) *Effectiveness:* compared with the conventional methods, the novel DL method can work for the high-contrast objects; 2) *Simplicity:* not only the DL framework avoids computing complex Green's functions and the high complexity of the conventional methods, but also the two-step process is very convenient to implement; 3) *Accuracy:* the precision of the newly proposed two-step approach is much better than the one-step based approaches.

The letter is organized as follows. In Section II, the formulation of EMIS is illustrated while the newly proposed model is

Manuscript received March 31, 2019; revised May 22, 2019; accepted June 5, 2019. Date of publication June 27, 2019; date of current version November 4, 2019. This work was supported in part by the Research Grants Council of Hong Kong under Grant GRF 17207114 and Grant GRF 17210815; in part by the Asian Office of Aerospace Research and Development (AOARD) under Grant FA2386-17-1-0010; in part by the National Natural Science Foundation (NSFC) under Grant 61271158; and in part by the Hong Kong University Grants Committee (UGC) under Grant AoE/P–04/08. *(Corresponding author: Lijun Jiang.)*

H. M. Yao and L. Jiang are with the Department of Electrical and Electronic Engineering, University of Hong Kong, Hong Kong (e-mail: yaohmhk@hku.hk; jianglj@hku.hk).

W. E. I. Sha is with the Key Laboratory of Micro-Nano Electronic Devices and Smart Systems of Zhejiang Province, College of Information Science and Electronic Engineering, Zhejiang University, Hangzhou 310027, China (e-mail: weisha@zju.edu.cn).

Digital Object Identifier 10.1109/LAWP.2019.2925578

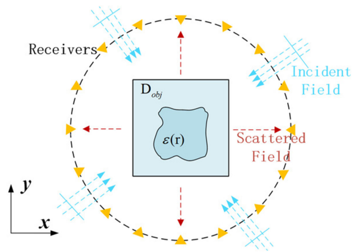


Fig. 1. Schematic of scattering of $\mathrm{TM}_z$ wave from a dielectric region $D_{obj}$.

described. The next section discusses the process of employing the proposed DL method to solve EMIS. In Section III, numerical benchmarks are provided to show the validity and accuracy of our proposed method. Last, the Section IV gives the conclusion.

## II. Problem and Formulation

### A. EMIS Formulation

The representative configuration for EMIS is shown in Fig. 1. This two-dimensional (2-D) application is used to demonstrate our methodology. However, our method is also suitable for 3-D situations. In Fig. 1, $D_{obj}$ denotes the investigated object domain. It is divided into $N \times N$ pieces. The 2-D $\mathrm{TM}_z$ wave is denoted as $E^{\mathrm{in}}$. The illuminated scattered field $E^s$ can be measured by $M$ receivers around the object. The entire forward process for EMIS is written by two governing equations, referred to as Lippmann–Schwinger equations [14], [33]. The first equation, denoted as the data equation, describes the scattered field as a reradiation by the field $E^t$ of scatterers in the object domain as

$$E^s(\boldsymbol{r}) = k_0^2 \int_{D_{obj}} G(\boldsymbol{r}, \boldsymbol{r}')\, \chi(\boldsymbol{r}')\, E^t(\boldsymbol{r}')\, d\boldsymbol{r}' \tag{1}$$

where $G(\boldsymbol{r}, \boldsymbol{r}')$ is the Green's function. For the $\mathrm{TM}_z$ wave, it is defined as $G(\boldsymbol{r}, \boldsymbol{r}') = -\frac{j}{4} H_0^{(2)}(k_0 |\boldsymbol{r} - \boldsymbol{r}'|)$. $H_0^{(2)}$ stands for the Hankel function of the zeroth order of the second kind and $k_0$ is the wavenumbers of the free space. $\boldsymbol{r}' = (x', y')$ is the source point in object domain, while $\boldsymbol{r} = (x_R, y_R)$ represents the position vector at the receiver. $E^t$ represents the total electronic field. The contrast function is defined as $\chi(\boldsymbol{r}') = \varepsilon_r(\boldsymbol{r}') - 1$.

The second equation for EMIS, usually called the state equation [33], describes the field interaction between scatterer pieces in object domain $D_{obj}$ as

$$E^t(\boldsymbol{r}) = E^{\mathrm{in}}(\boldsymbol{r}) + k_0^2 \int_{D_{obj}} G(\boldsymbol{r}, \boldsymbol{r}')\, \chi(\boldsymbol{r}')\, E^t(\boldsymbol{r}')\, d\boldsymbol{r}' \tag{2}$$

where $\boldsymbol{r} = (x, y)$ and $\boldsymbol{r}' = (x', y')$ are, respectively, the field and source points.

The final goal of EMIS problems is to reconstruct the relative permittivities $\varepsilon_r$ (or $\chi$) of scatterers from $E^s$ in object domain $D_{obj}$. In conventional methods, the object domain $D_{obj}$ is uniformly discretized into pieces where the total electric fields and the contrast functions are also considered piece-wise constant. Ultimately, the solving process of EMIS is to transfer (1) and (2) into the following coupled equations in discretized form [7], [34]:

$$\bar{E}^s = \bar{\bar{G}}_R \cdot \mathrm{diag}\left(\bar{E}^t\right) \cdot \bar{\chi} \tag{3}$$

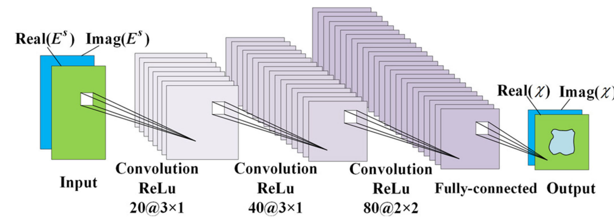


Fig. 2. DConvNet architecture for the first step.

$$\bar{E}^t = \bar{E}^{\mathrm{in}} + \bar{\bar{G}}_D \cdot \mathrm{diag}\left(\bar{E}^t\right) \cdot \bar{\chi} \tag{4}$$

where $\bar{\bar{G}}_R$ and $\bar{\bar{G}}_D$ are the discretized Green's function in (1) and (2).

In conventional methods, instead of directly solving the coupled equations, an objective function $f(\chi)$ is constructed for optimization in (5). However, obtaining contrast from (5) is a very difficult nonlinear process [14]

$$\min: \ f(\chi) = \sum_{i=1}^{N_i} E_i^s - E_i^s(\chi)' + \alpha D(\chi) \tag{5}$$

where the measured scattered field $E_i^s$ caused by $N_i$ different incident field $E^{\mathrm{in}}$ is approached by the optimized scattered fields $E_i^s(\chi)'$ by iteration computation of (5). $D$ is the specified sparse transformation, such as the wavelet transformation [35].

### B. Two-Step Deep Learning Approach

To solve the high contrast problem with high accuracy, a two-step DL approach is proposed to solve the EMIS problem. In our approach, complex-valued convolutional neural network models are utilized to convert original scattered fields into the permitivitties of scatterers in object domain. Regarded as the straightforward extension of the conventional real-valued CNN, the complex-valued CNN is naturally closer to the problem formulation for the EMIS problem, and it can allow for richer information to be captured from the input space [26], [36], [37]. Because the requirement of the huge number of training samples is difficult to fulfill by real experiment, we use simulation data to train the DL models. The designed architecture of the proposed approach for solving EMIS is formulated into the following two steps.

*Step 1:* Retrieve the initial contrast by DConvNet

The first step can be regarded as a "heterogeneous" process, which transfers measured scattered field into a preliminary contrast of the object domain. This step is based on the complex-valued DConvNet, which employs original scattered fields $E^s$ as the input and the ground-truthed contrast $\chi$ of scatterer as the output. Typical ConvNets [38], [39] consists of four types of layers: input layers, convolutional layers, pooling layers, and fully connected layers. By stacking these layers together, a typical ConvNet structure is formed. In this letter, we utilize these typical layers to form our DConvNet model for the first "heterogeneous" step.

The internal architecture of the proposed DConvNet is shown in Fig. 2. The inputs are the $M \times N_i \times 2$ matrix transferred from the scattered field use $E^s$, denoted as "field data," where $M$ stands for $M$ receivers, $N_i$ represents the number of incident fields, and the real and imaginary parts of $E^s$ act as its two tubes, as shown in Fig. 3. The corresponding outputs are the

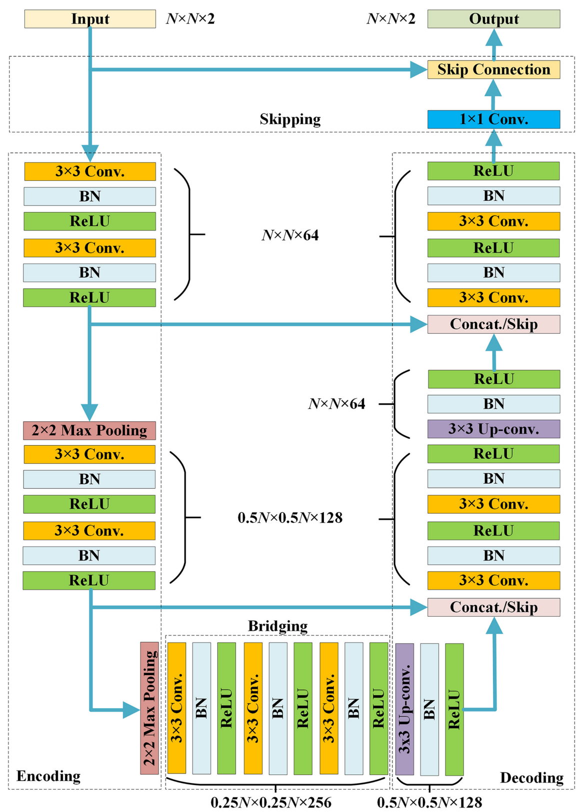


Fig. 3. DRCNN architecture for the second step.

TABLE I
DConvNet Architecture

| Type | Filter Number | Filter Size | Stride | Input Size | Output Size |
|---|---|---|---|---|---|
| Convolution | 20 | 3×1 | [2, 1] | $M\times N_i\times 2$ | $(M/2)\times N_i\times 20$ |
| ReLU | | | | $(M/2)\times N_i\times 20$ | $(M/2)\times N_i\times 20$ |
| Convolution | 40 | 3×1 | [2, 1] | $(M/2)\times N_i\times 20$ | $(M/4)\times N_i\times 40$ |
| ReLU | | | | $(M/4)\times N_i\times 40$ | $(M/4)\times N_i\times 40$ |
| Convolution | 80 | 2×2 | [1, 1] | $(M/4)\times N_i\times 40$ | $(M/4)\times N_i\times 80$ |
| ReLU | | | | $(M/4)\times N_i\times 80$ | $(M/4)\times N_i\times 80$ |
| Fully-connected | | | | $(M/4)\times N_i\times 80$ | $M\times N_i\times 20$ |
| Regression Loss function | | | | $M\times N_i\times 20$ | $N\times N\times 2$ |

$N \times N \times 2$ matrix consisting of the real and imaginary parts of the objective contrast. Thus, the relationship between the input and output can be expressed by the (6), where $\Gamma$ stands for the nonlinear operation of DConvNet in the first step

$$\chi = \Gamma\left(E^s\right). \tag{6}$$

The convolutional layer and activation layer unit operate to capture features of input. Convolutional layer number, kernel number $f$, its size $K$, and the stride for kernel are shown in Table I. Then, this convolutional layer and activation layer unit feed into a final fully-connected layer, which predicts the contrast $\chi$. This final output is used to compute the half-mean-squared error between the true label and the predicted label, referred to as the loss.

The DConvNet model for the first step is benchmarked in MATLAB 2019a with a Deep Learning Toolbox [40]. An adaptive moment estimation (Adam) optimizer is chosen to optimize the half-mean-squared-error loss function. The Adam optimizer can navigate through the loss surface more successfully than other optimizer, such as Stochastic Gradient Descent [41]. Moreover, 0.2 dropout regularization is applied to reduce or prevent over-fitting and to improve prediction accuracy. Unfortunately, due to the limited measured field information, though the DConvNet in this step can roughly realize the reconstruction of contrast, its precision cannot still fulfill the requirement of engineering application [7], [25]–[27], [32]–[34]. Thus, the first step acts as the initial value choosing process of some conventional methods, such as a Born iterative method, which requires a roughly approximated initial value for future optimization [9].

*Step 2:* Refining the initial contrast by DRCNN

The next step can be concluded as a "homogenous" process, which improves the originally reconstructed contrast to the accurate final result. In this step, the complex-valued DRCNN is employed to use the retrieved initial contrast obtained in the first step as the new input to realize the refinement.

The input of the DRCNN is the coarsely reconstructed contrast $\chi$ obtained from the first step, while the corresponding ground-truthed contrast $\chi$ acts as the output. The size of input and output are both $N \times N \times 2$, composing of the real and imaginary parts of the contrast. The proposed DRCNN is modified based on the architecture of U-Net [42], which has been widely employed for segmentation. The U-net CNN architecture is well suited for the EMIS problem. First, its downsampling operation in contracting path greatly increases the effective receptive field of the network and greatly enhance the prediction at each pixel of the output image [43]. Besides, its batch normalization (BN) structure greatly alleviates the internal covariate shift by the normalization step, and thus, BN increases its robustness to initializations [44]. Such as [25]–[28], the paramount parameters of the proposed DRCNN are shown in Fig. 3. The proposed DRCNN comprises of four parts: encoding, bridging, decoding, and skipping, shown in Fig. 3. The first part encodes the input contrast "image" into compact representations, while the corresponding decoding part recovers the representations. The middle bridging part acts as the bridge connecting the encoding and decoding paths. Plus, the skip connection for residual learning is added into the last part, implemented between the input of the neural network and the output layer in our modified U-net structure. The added skip connection means that our model actually learns the difference between input and output. The encoding part is equipped with repeated application of $3 \times 3$ convolution, BN, and rectified linear unit (ReLU) and $2 \times 2$ max-pooling operation. Meanwhile, the decoding part is armed with the repeated application of $3 \times 3$ up-convolution, BN, ReLU, and concatenation operation with skip connection, as shown in Fig. 3.

Our model above was built with the following special modifications.

1) *Skip connection:* unlike the conventional U-Net [42], the skip connection is added into our DRCNN. The skip connection enables the entire network to learn the difference between the rough contrast "image" from the first step and the ground-truthed contrast "image," i.e., adding the residual learning function to the proposed model. Besides, the added skip connection can effectively avoid the vanishing gradient problem in the training process [45]. Different from the same network without the skip connection, its implementation can bring a noticeable improvement in performance [27], [28].

2) *Complex-valued input and output:* considering the EMIS problem is a typical complex-valued problem, we modify the

input and output channel number of the original U-Net [42]. As a result, their real part and imaginary parts can be adapted in different channel. Thus, our proposed model is more flexible and adaptable for the contrast reconstruction for the real application scenario.

Hence, the second step acts as the iterative refining process of most conventional iterative optimization methods [6]–[13], which refine the contrast by optimization. We also emphasize that the entire model construction process never depends on the Green's function computation. Plus, our method can help to reduce ill conditioned systems that conventional methods usually deal with [46]. The relationship of the entire process can be expressed as (7), where $\mathcal{F}$ represents the nonlinear operation of the DRCNN. In the second step, the Adam optimizer is still chosen to optimize the half-mean-squared-error loss function, while 0.2 dropout regularization is used to reduce overfitting in the proposed DRCNN

$$\chi = \mathcal{F}\left(\Gamma\left(E^{s}\right)\right). \tag{7}$$

In conclusion, the first step acts as the initial value choosing process of some conventional methods, while the second step acts as the iterative refining process of most conventional iterative methods. The proposed two steps perfectly replace the process of conventional methods for solving the EMIS problem.

## III. Numerical Results

In this section, the MNIST dataset is chosen to verify the effectiveness and accuracy of the proposed two-step DL approach. Individual samples in MNIST dataset with the size of 2λ × 2λ (λ = 1 m in free space) are discretized into 28 × 28 even pieces ($N = 28$). Besides, six different incident plane waves with incident angle evenly distributed within [0°, 360°) are exerted to object domain $D_{obj}$, separately $(N_i = 6)$. $M = 20$ receivers are evenly located around the object domain $D_{obj}$ with the distance 30λ. The full-wave EM simulations [47] are used on all samples to generate training and testing data. Based on MNIST [25]–[27], the number-shaped objects are set to the extremely high contrast with the relative permittivity $\varepsilon_r = 8$, which is considered as a very challenging case. To ensure the generalization, we randomly choose 8000 samples in MNIST dataset for training DL models of the proposed two-step approach. According to our trail, the performance of the trained models based on the same number of randomly chooses samples keeps stable. Another 1000 samples are chosen for testing. To evaluate the quality of reconstructed "images," we normalize the results and employ mean-square error (MSE) of the normalized result as the quantitative indicator, as done in [23]–[27]. Moreover, as the comparison, the Born iterative method is also employed to reconstruct the contrast of testing samples. The results have been shown in Fig. 4.

From Fig. 4, we can see the ground truths of testing samples, reconstructed images from the Born iterative method [9], the reconstructed results from the first and second step of our proposed DL approach. Clearly the final outputs of the proposed method are much better reconstruction of the ground truth. However, the first step can only provide coarsely reconstructed objects. For this high-contrast case, the Born iterative method cannot produce any meaningful result.

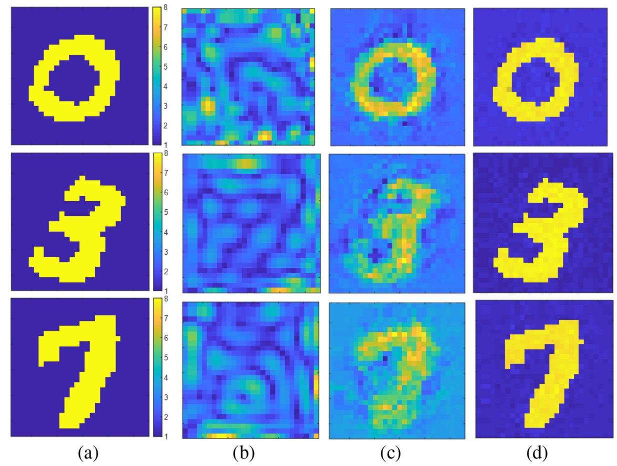


Fig. 4. Comparison of reconstructed relative permittivity of number-shaped objects. (a) Ground truths. (b) Reconstructed relative permittivity from the Born iterative method. (c) Reconstructed rough relative permittivity from the first step of the proposed approach. (d) Reconstructed final relative permittivity from the second step of the proposed approach.

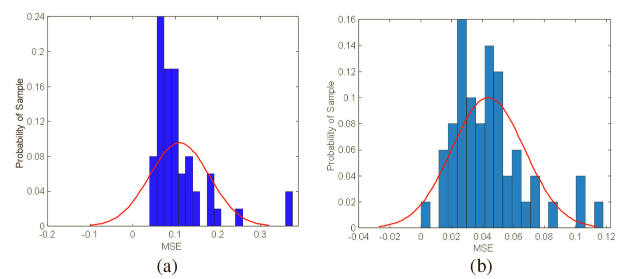


Fig. 5. MSE statistical histograms of the normalized reconstructed contrast "image" quality. (a) Results obtained from the first step of the proposed approach. (b) Results obtained from the second step of the proposed approach.

Fig. 5 shows the statistical analysis of the testing results, where the MSE average of normalized reconstructed results by the proposed method are about 0.04, while that average obtained from the first step can even overcome 0.1. Hence, the proposed two-step DL approach can solve the EMIS problem with a much better performance.

## IV. Conclusion

This letter proposes a new two-step DL approach to solve EMIS problems. These two steps implement the "heterogeneous" and "homogeneous" reconstruction process, respectively. The contrast of scatterers can be reconstructed with the enhanced refinement. In the first step, a complex-valued DConvNet is employed to extract the initial contrast from measured field data. In the second step, the retrieved initial is further enhanced by a complex-valued deep residual network (DRCNN) to realize the reconstruction improvement. Consequently, the EMIS problems can be solved with much higher accuracy even for high-contrast objects. Numerical examples demonstrate the capability and feasibility of the proposed method with the clear accuracy improvement. The proposed DL approach for the EMIS problem provides a new thinking in realizing real-time quantitative microwave imaging.

## REFERENCES


[1] P. M. Meaney, M. W. Fanning, D. Li, S. P. Poplack, and K. D. Paulsen, "A clinical prototype for active microwave imaging of the breast," *IEEE Trans. Microw. Theory Tech.*, vol. 48, no. 11, pp. 1841–1853, Nov. 2000.

[2] M. Pastorino, *Microwave Imaging*. New York, NY, USA: Wiley, 2010.

[3] G. Maire *et al.*, "Experimental demonstration of quantitative imaging beyond Abbe's limit with optical diffraction tomography," *Phys. Rev. Lett.*, vol. 102, May 2009, Art. no. 213905.

[4] O. Bucci and T. Isernia, "Electromagnetic inverse scattering: Retrievable information and measurement strategies," *Radio Sci.*, vol. 32, no. 6, pp. 2123–2137, 1997.

[5] L. Neira, B. van Veen, and S. Hagness, "High-resolution microwave breast imaging using a 3-d inverse scattering algorithm with a variable-strength spatial prior constraint," *IEEE Trans. Antennas Propag.*, vol. 65, no. 11, pp. 6002–6014, Nov. 2017.

[6] P. Rocca *et al.*, "Evolutionary optimization as applied to inverse problems," *Inverse Problems*, vol. 25, pp. 1–41, Dec. 2009.

[7] P. Rocca, G. Oliveri, and A. Massa, "Differential evolution as applied to electromagnetics," *IEEE Antennas Propag. Mag.*, vol. 53, no. 1, pp. 38–49, Feb. 2011.

[8] J. Robinson and Y. Rahmat-Samii, "Particle swarm optimization in electromagnetics," *IEEE Trans. Antennas Propag.*, vol. 52, no. 2, pp. 397–407, Feb. 2004.

[9] M. Moghaddam and W. C. Chew, "Study of some practical issues in inversion with the born iterative method using time-domain data," *IEEE Trans. Antennas Propag.*, vol. 41, no. 2, pp. 177–184, Feb. 1993.

[10] A. Abubakar and P. Berg, "The contrast source inversion method for location and shape reconstructions," *Inverse Problems*, vol. 18, no. 2, pp. 495–510, 2002.

[11] K. Agarwal, R. Song, M. D'Urso, and X. Chen, "Improving the performances of the contrast source extended born inversion method by subspace techniques," *IEEE Geosci. Remote Sens. Lett.*, vol. 10, no. 2, pp. 391–395, Mar. 2013.

[12] L. Crocco, M. D'Urso, and T. Isernia, "Testing the contrast source extended born inversion method against real data: The TM case," *Inverse Problems*, vol. 21, 2005, Art. no. S33.

[13] X. Chen, "Subspace-based optimization method for solving inverse scattering problems," *IEEE Trans. Geosci. Remote Sens.*, vol. 48, no. 1, pp. 42–49, Aug. 2010.

[14] X. Chen, *Computational Methods for Electromagnetic Inverse Scattering*. Hoboken, NJ, USA: Wiley, 2018.

[15] C. M. Bishop, *Pattern Recognition and Machine Learning*. New York, NY, USA: Springer, Aug. 2006.

[16] H. M. Yao, L. J. Jiang, and Y. W. Qin, "Machine learning based method of moments (ML-MoM)," in *Proc. Int. Symp. IEEE Antennas Propag. USNC/URSI Nat. Radio Sci. Meeting*, San Diego, CA, 2017, pp. 973–974, doi: 10.1109/APUSNCURSINRSM.2017.8072529.

[17] W. Tang *et al.*, "Study on a Poisson's equation solver based on deep learning technique," in *Proc. Int. Symp. IEEE Elect. Des. Adv. Packag. Syst.*, Haining, China, 2017, pp. 1–3. doi: 10.1109/EDAPS.2017.8277017.

[18] H. M. Yao, W. E. I. Sha, and L. J. Jiang, "Applying convolutional neural networks for the source reconstruction," *Progress Electromagn. Res. M*, vol. 76, pp. 91–99, 2018, doi: 10.2528/PIERM18082907.

[19] Z. Lin, K. Ji, M. Kang, X. Leng, and H. Zou, "Deep convolutional highway unit network for SAR target classification with limited labeled training data," *IEEE Geosci. Remote Sens. Lett.*, vol. 14, no. 7, pp. 1091–1095, Jul. 2017.

[20] S. Z. Chen, H. P. Wang, F. Xu, and Y. Q. Jin, "Target classification using the deep convolutional networks for SAR images," *IEEE Trans. Geosci. Remote. Sens.*, vol. 54, no. 8, pp. 4806–4817, Aug. 2016.

[21] H. H. Zhang, H. M. Yao, and L. J. Jiang, "Embedding the behavior macromodel into TDIE for transient field-circuit simulations," *IEEE Trans. Antennas Propag.*, vol. 64, no. 7, pp. 3233–3238, Jul. 2016.

[22] H. H. Zhang, L. J. Jiang, H. M. Yao, and Y. Zhang, "Transient heterogeneous electromagnetic simulation with DGTD and behavioral macromodel," *IEEE Trans. Electromagn. Compat.*, vol. 59, no. 4, pp. 1152–1160, Aug. 2017.

[23] S. Caorsi and P. Gamba, "Electromagnetic detection of dielectric cylinders by a neural network approach," *IEEE Trans. Geosci. Remote Sens.*, vol. 37, no. 2, pp. 820–827, Mar. 1999.

[24] I. T. Rekanos, "Inverse scattering of dielectric cylinders by using radial basis function neural networks," *Radio Sci.*, vol. 36, no. 5, pp. 841–849, 2001.

[25] L. Li, L. G. Wang, and F. L. Teixeira, "Performance analysis and dynamic evolution of deep convolutional neural network for nonlinear inverse scattering," 2019. [Online]. Available: https://arxiv.org/abs/1901.02610

[26] L. Li, L. G. Wang, F. L. Teixeira, C. Liu, A. Nehorai, and T. J. Cui, "DeepNIS: Deep neural network for nonlinear electromagnetic inverse scattering," *IEEE Trans. Antennas Propag.*, vol. 67, no. 3, pp. 1819–1825, Mar. 2019.

[27] Z. Wei and X. Chen, "Deep-learning schemes for full-wave nonlinear inverse scattering problems," *IEEE Trans. Geosci. Remote Sens.,* vol. 57, no. 4, pp. 1849–1860, Apr. 2019. doi: 10.1109/TGRS.2018.2869221.

[28] K. H. Jin *et al.*, "Deep convolutional neural network for inverse problems in imaging," *IEEE Trans. Image Process.*, vol. 26, no. 9, pp. 4509–4522, Sep. 2017.

[29] Y. Sun *et al.*, "Efficient and accurate inversion of multiple scattering with deep learning," *Opt. Express*, vol. 26, no. 11, pp. 14678–14688, Apr. 2018.

[30] S. J. Hamilton and A. Hauptmann, "Deep D-bar: Real-time electrical impedance tomography imaging with deep neural networks," *IEEE Trans. Med. Imag.*, vol. 37, no. 10, pp. 2367–2377, Oct. 2018.

[31] A. Massa *et al.*, "Learning-by-examples techniques as applied to electromagnetics," *J. Electromagn. Waves Appl.*, vol. 32, no. 4, pp. 516–541, 2018.

[32] K. Belkebir, P. C. Chaumet, and A. Sentenac, "Superresolution in total internal reflection tomography," *J. Opt. Soc. Amer. A, Opt. Image Sci.*, vol. 22, no. 9, pp. 1889–1897, 2005.

[33] M. A. Fiddy and R. S. Ritter, *Introduction to Imaging From Scattered Fields*. Boca Raton, FL, USA: CRC Press, 2014.

[34] W. C. Chew and Y. M. Wang, "Reconstruction of two-dimensional permittivity distribution using the distorted Born iterative method," *IEEE Trans. Med. Imag.*, vol. 9, no. 2, pp. 218–225, Jun. 1990.

[35] A. L. da Cunha, J. Zhou, and M. N. Do, "The nonsubsampled contourlet transform: Theory, design, and applications," *IEEE Trans. Image Process.*, vol. 15, no. 10, pp. 3089–3101, Oct. 2006.

[36] C. Dong, C. C. Loy, K. He, and X. Tang, "Image super-resolution using deep convolutional networks," *IEEE Trans. Pattern Anal. Mach. Intell.*, vol. 38, no. 2, pp. 295–307, Feb. 2016.

[37] L. G. Wang, M. Wang, W. Zhong, and L. Li, "Complex-valued deep convolutional networks for nonlinear electromagnetic inverse scattering," in *Proc. Int. Conf. IEEE Comput. Electromagn.*, Chengdu, China, 2018, pp. 1–2.

[38] A. Krizhevsky, I. Sutskever, and G. Hinton, "Imagenet classification with deep convolutional neural networks," *Commun. ACM*, vol. 60, no. 6, pp. 84–90, 2017.

[39] Y. Zhang, D. Zhao, J. Sun, G. Zou, and W. Li, "Adaptive convolutional neural network and its application in face recognition," *Neural Process. Lett.*, vol. 43, no. 2, pp. 389–399, 2015.

[40] P. Kim, *MATLAB Deep Learning*, New York, NY, USA: Apress, 2017.

[41] D. P. Kingma and J. L. Ba, "Adam: A method for stochastic optimization," in *Proc. Int. Conf. Learn. Represent.*, 2015, pp. 1–41.

[42] O. Ronneberger, P. Fischer, and T. Brox, "U-net: Convolutional networks for biomedical image segmentation," in *Proc. 18th Int. Conf. Med. Image Comput. Comput.-Assist. Intervention*, 2015, pp. 234–241.

[43] J. Johnson *et al.*, "Perceptual losses for real-time style transfer and super-resolution," in *Proc. Eur. Conf. Comput. Vis.*, 2016, pp. 694–711.

[44] S. Ioffe and C. Szegedy, "Batch normalization: Accelerating deep network training by reducing internal covariate shift," in *Proc. Int. Conf. Mach. Learn.*, 2015, pp. 448–456.

[45] K. He, X. Zhang, S. Ren, and J. Sun, "Deep residual learning for image recognition," in *Proc. Int. Conf. IEEE Comput. Vis. Pattern Recognit.*, Jun. 2016, pp. 770–778.

[46] J. K. Seo *et al.*, "A learning-based method for solving ill-posed nonlinear inverse problems: A simulation study of lung EIT," 2019. [Online]. Available: https://arxiv.org/abs/1810.10112

[47] M. F. Catedra, R. P. Torres, J. Basterrechea, and E. Gago, *The CG-FFT Method: Application of Signal Processing Techniques to Electromagnetics*. Boston, MA, USA: Artech House, 1995.